International Journal of Energy Research

INTERNATIONAL JOURNAL OF ENERGY RESEARCH
Int. J. Energy Res. 2012; **36**:963–974
Published online 29 March 2011 in Wiley Online Library (wileyonlinelibrary.com). DOI: 10.1002/er.1848

Experimental and theoretical study of an integrated thermoelectric–photovoltaic system for air dehumidification and fresh water production

M. Jradi, N. Ghaddar*,† and K. Ghali

Department of Mechanical Engineering, American University of Beirut, P.O. Box 11-0236, Beirut 1107-2020, Lebanon

SUMMARY

The main objective of this study is to present an integrated thermoelectric–photovoltaic renewable system to dehumidify air and produce fresh water. The system is combined with a solar distiller humidifying ambient air to enhance distillate output to meet the specified fresh water needs for a residential application.

A model is developed to simulate the air dehumidification process using thermoelectrically cooled TEC channels. Experiments were performed to validate the developed model results. It is found that the model predicted well the variation in the air temperature along the channel with a maximum relative error in air temperature less than 2.4%. In addition, the simulation model predicted well the amount of water condensate produced by the integrated system with a maximum relative error of 8.3%.

An optimization problem is formulated to design and set the integrated system optimal operation to produce 10 L of fresh water per day meeting the fresh water needs of a typical residential. Using five TEC channels of a length of 1.2 m and an area of $0.07 \times .05\,m^2$ integrated with 1.2-m^2 solar distiller that recirculates a constant air mass flow rate of $0.15\,kg\,s^{-1}$ is capable of meeting water demand when air mass flow rate through each TEC channel is optimally set at $0.0155\,kg\,s^{-1}$. The associated optimal electrical current input to the TEC modules varied depending on the month and is set at 2.2 A in June, 2.1 A in July and 2.0 A in August, September and October. Copyright © 2011 John Wiley & Sons, Ltd.

KEY WORDS

thermoelectric–photovoltaic water production system; thermoelectric cooling; humidification/dehumidification process; fresh water production; design and optimization of the thermoelectric–photovoltaic system

Correspondence

*N. Ghaddar, American University of Beirut, P.O. Box 11-236, Riad El Solh, Beirut 1107-2020, Lebanon.
†E-mail: farah@aub.edu.lb

Received 16 December 2010; Revised 2 February 2011; Accepted 10 February 2011

1. INTRODUCTION

Despite the technological and the industrial advancement, the lack of fresh water resources emerges as one of the critical problems threatening the humanity. Recent statistics show that about 15% of the people in the Arab World do not have access to clean and fresh water, and this percentage is expected to increase in the upcoming years [1]. The warm and dry climates in the Middle East and North Africa exhibit the severest fresh water scarcity problem due to the increase in the salinity rate of the ground water and the sporadic rainfall [2]. This raises the need for environmental friendly solutions including fresh water extraction from the atmosphere while utilizing renewable resources. Using photovoltaic (PV)-powered thermoelectrically cooled surfaces to extract water from the atmosphere is one viable solution that takes advantage of the humid climate prevailing in many areas of the Middle East most of the year. In the days when air humidity is, the power consumption of thermoelectric cooling modules would drastically increase which means that other methods are to be sought to humidify ambient air. Integrating a solar distiller with a thermoelectric cooling system would increase the water content of the air into the cooling system to produce the desired fresh water at lower electrical power consumption.

Considerable amount of research has been conducted in the field of thermoelectric cooling to predict and optimize the performance of thermoelectric modules [3–11]. Huang *et al.* reported that the two major factors for enhancing the efficiency of the thermoelectric modules are the heat sink thermal resistance and the appropriate cooling capacity to reach optimal performance [3]. Similar study reported by Chang *et al.* [12]

who found that for a given heating load, there is a corresponding optimal current for the module, and that the thermoelectric modules become more effective at lower heat loads. Cosnier *et al.* [13] presented an experimental and analytical study for a thermoelectric system for air pre-cooling and pre-heating and found that the system could be feasible and efficient reaching a coefficient of performance (COP) of 1.5 in the cooling mode and about 2 in the heating mode. This can be achieved by supplying an optimal current to the modules and maintaining a desirable temperature difference of using a proper heat sink. Furthermore, several studies investigated the viability of using PV solar panels to supply the thermoelectric cooling modules. Gillot *et al.* [14] used thermoelectric modules for small-scale space conditioning and built a system prototype that consisted of eight cooling modules to generate a cooling capacity up to 220 W with a COP of 0.46 under current input of 4.6 A. They found that the use of solar PV to feed the thermoelectric modules would be competitive and feasible if the PV's price is lower than £1.25 W^{-1}. Dai *et al.* [15] investigated the viability of building a thermoelectric refrigerator driven by solar PV cells to serve people in remote and rural areas and proposed refrigerator temperature ranges between 5 and 10°C at a COP of about 0.3.

Thermoelectric dehumidification was examined by very few researchers. One study was conducted by Vian *et al.* [16] who developed a small dehumidifier prototype made up of three thermoelectric cooling modules and a computational model (AERO) was used for the design and the optimization of the modules' performance. Their system consumed 100 W at optimum conditions of 27°C and 82% relative humidity with a COP, which was much lower than the vapor-compression devices.

The aim of this study is to design a solar-driven thermoelectric cooling system integrated with solar distiller for air dehumidification and fresh water production. The study will concentrate on studying the viability of applying thermoelectric technology in designing a low-power dehumidifying device driven by solar PV panels to generate fresh water in the Lebanese coastal humid climate. A robust model will be developed to simulate the dehumidification of the humid air through the thermoelectrically cooled channel surface and to predict the thermal and the electrical performance of the modules as well as the amount of condensate generated. A TEC channel prototype will be built and experiments will be carried out to validate the model predictions of the amount of water condensate collected and the other system performance parameters. A case study will be presented to assess the integrated dehumidification system in achieving the objectives of meeting the desired fresh water needs in the Lebanese humid climate.

2. SYSTEM DESCRIPTION AND PROBLEM STATEMENT

Figure 1 depicts the PV-powered thermoelectric cooled channel integrated with a solar distiller. The system is composed of three major elements: thermoelectric cooled channel per second, the PV solar panels and

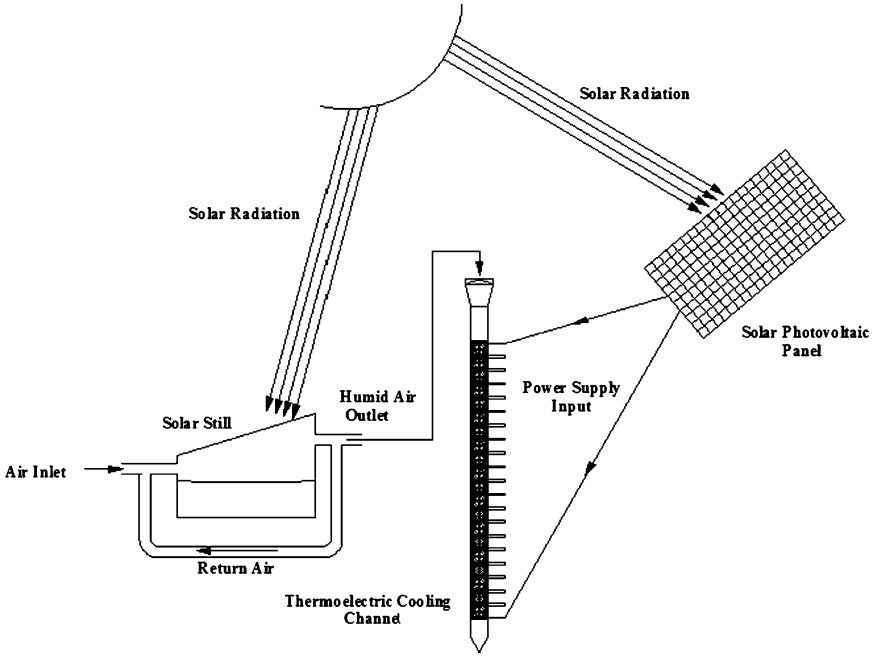

Figure 1. General sketch for the integrated system units.

Int. J. Energy Res. 2012; **36**:963–974 © 2011 John Wiley & Sons, Ltd.
DOI: 10.1002/er

the solar distiller humidification unit. The cooling channel is sized such that one side of the channel is cooled by thermoelectric modules and the other sides are assumed well insulated. The thermoelectric cooling modules are fed directly by a direct current (DC) electric power supply and play the role of a heat pump; thus extracting heat from the air flowing along the channel at the cold side of the thermoelectric cooling modules and rejecting this heat at the other side of the modules. The PV panels serve as a renewable electricity supply source. Since the equipped thermoelectric modules need a DC electric power supply source to operate, then the PV modules make an appropriate renewable solution for feeding the thermoelectric modules with the sufficient electric power needed to pump the desired cooling capacity. Since the system is proposed to produce fresh water in humid climates, then a humid air source is needed to supply the thermoelectric channel with the desired humid air inlet. The solar distiller can play the role of increasing the water content of the air entering the channel in order to produce the larger amount of condensed water.

Ambient air is humidified by the solar distiller and then dehumidified by the thermoelectric cooling modules to extract water condensate and generate the needed fresh water. The main parameters governing the integrated system operation are

- Electric current feed to the thermoelectric module (I).
- Mass flow rate of the supply air to the thermoelectric cooling channel ($\dot{m}$).
- Temperature and humidity ratio of the air entering the thermoelectric cooling channel (T_{a-in} and w_{a-in}).
- Ambient air conditions controlling the operation of the system (T_{amb} and w_{amb}).
- Output air temperature and humidity ratio from the solar distiller (T_{a-dist} and w_{a-dist}).

In the first part of the methodology section, the thermoelectric cooling channel air and moisture thermal transport model is presented followed by the description of experimental methodology to validate the model predictions of the water condensate collected and other system performance parameters.

3. MATHEMATICAL FORMULATION

The thermoelectric cooling module is characterized by four parameters describing its maximal performance, which are: the maximum temperature difference between the hot side and the cold side of the thermoelectric module ΔT_{max}, the maximal pumping cooling capacity at the cold side corresponding to zero temperature difference across the thermoelectric module Q_{max}, the maximum voltage difference which can be applied to the thermoelectric module with the absence of any heat load U_{max} and the maximal operational input current to the thermoelectric module at the maximum temperature difference I_{max}. Each TEC module is treated as a lumped surface represented by uniform value for each of its operational parameters, The basic operational characteristics of a thermoelectric module include the cold side temperature (T_c), the hot side temperature (T_h), the heat pumping capacity at the cold side (Q_c), the heat dissipated at the hot side (Q_h), the electric current (I) and the voltage difference (U). The modeling of the TEC module will follow the derivations of Tsai *et al.* [17] where the operation and the performance of the module is governed by three main energy processes namely the Joule's effect, the Peltier cooling effect and the thermal conduction.

The heat cooling capacity at the cold side and the heat dissipated at the hot side can be obtained by applying steady-state energy balances for both sides of the thermoelectric cooling module [18]. As a result, the heat pumping cooling capacity at the cold side of the thermoelectric cooling module is given by:

$$Q_c = \alpha I T_c - \frac{1}{2} I^2 R_e - k(T_h - T_c) \quad (1)$$

where I is the electric current in A, R_e is the electrical resistivity of the module in ohm, α is the Seebeck coefficient of the module in V/K, k is the thermal conductance in W/K and $T_{c/h}$ is the cold/hot side temperature [19]. The heat dissipated at the hot side of the thermoelectric module is given by

$$Q_h = \alpha I T_h - \frac{1}{2} I^2 R_e - k(T_h - T_c) \quad (2)$$

This heat dissipated is the sum of both the heat pumping capacity at the cold side of the module and the electric power input to the module. In addition, the input voltage difference applied to the thermoelectric module is given by

$$U = \alpha\,(T_h - T_c) + I\,R_e \quad (3)$$

The electric power consumption of the thermoelectric module is given by

$$P = U \times I = \alpha\, I\,(T_h - T_c) + I^2\, R_e \quad (4)$$

The COP is defined as the cooling heat capacity pumped by the thermoelectric module divided by the electric power consumption of the module. The overall characteristics of the thermoelectric modules are given in terms of the characteristics of one thermoelectric element as follows:

$$\alpha = \alpha\_e \times \mathrm{Nb} \times 2 \quad (5a)$$

$$R_e = \frac{R_e\_e \times \mathrm{Nb} \times 2}{\mathrm{Gf}} \quad (5b)$$

$$k = k\_e \times \mathrm{Nb} \times 2 \times Gf \quad (5c)$$

where Nb is the number of thermocouples in the thermoelectric cooling module, Gf is the geometry

factor of the thermoelectric element, α_e is the Seebeck coefficient for one thermoelectric element in V/K, R_{e_e} is the electrical resistivity of a thermoelectric element in W/K and k_e is the total thermal conductance for one element in W/K. For bismuth telluride thermoelectric cooling modules and using the correlations of Gillot *et al.* [14], the Seebeck coefficient, the electrical resistivity and the total thermal conductance for a single thermoelectric element are expressed in terms of the average thermoelectric cooling module temperature T_m in degree Kelvin as follows:

$$\alpha\_e = (-0.45263 + 0.01424 \times T_m - 2.02517 \times 10^{-5} \times T_m^2) \times 10^{-4} \quad (6a)$$

$$R_{e\_e} = (-5.57299 + 0.06035 \times T_m - 2.38881 \times 10^{-5} \times T_m^2) \times 10^{-4} \quad (6b)$$

$$k\_e = \begin{pmatrix} 5.06021 - 0.04244 \times T_m \\ +1.96459 \times 10^{-4} \times T_m^2 \\ -4.19064 \times 10^{-7} \times T_m^3 \\ +3.4922 \times 10^{-10} \times T_m^4 \end{pmatrix} \times 10^{-2} \quad (6c)$$

where T_m is the average temperature of the thermoelectric cooling module in degrees Kelvin.

The channel cooled surface by each TEC module is assumed isothermal at the temperature of associated module. Each module is considered independent from the other modules. The air flow in the channel is modeled as 1-D fully developed flow considering that the channel width is much smaller than its length. There will be an initial length of the channel where sensible cooling will take place until the TE module cold surface temperature is equal to the dew point of the passing air flow. Once dew point is reached at the surface, it is treated as wet over the rest of the modules in the channel [20]. The pumping cooling capacity at the cold module side is given by rate of enthalpy change given by

$$Q_c = \dot{m} \times (h_{a-in} - h_{a-out}) \quad (7)$$

where $\dot{m}$ is the air mass flow rate, h_{a-in} and h_{a-out} are the enthalpies of the air at inlet and exit of each module part of the channel. The heat dissipated at the hot side is given by

$$Q_h = \frac{(T_h - T_{amb})}{R_0} \quad (8)$$

where T_{amb} is the ambient air temperature, R_0 is the overall thermal resistance on the hot side. The variation in air temperature over the dry part of the channel for each module sector of the channel is given by

$$\frac{T_{a-in} - T_c}{T_{a-out} - T_c} = \exp\left(-\frac{Ah_I}{\dot{m}c_p}\right) \quad (9a)$$

The variation in the air enthalpy along each of all the wet modules is given by

$$\frac{h_{a-in} - h_{surface}}{h_{a-out} - h_{surface}} = \exp\left(-\frac{Ah_i}{\dot{m}c_p}\right) \quad (9b)$$

where C_p is the specific heat capacity in $J\,kg^{-1}\,K^{-1}$, A is the cooled surface area, h_i is the overall internal convective heat coefficient inside the duct which is calculated and updated in both dry and wet conditions, T_{a-in} and T_{a-out} are the temperatures of inlet and exit air flow of the ducted module while h_{a-in} and h_{a-out} are the enthalpies of inlet and exit air flow of the wet-ducted module, and $h_{surface}$ is the saturation enthalpy of the flowing air at the cold surface temperature. The workable range of air flow in the TEC channel for dehumidification to take place corresponds to transitional and turbulent flow ranging from 5000 to 20 000 based on the hydraulic diameter. By design, almost half of the channel length will be dry and the rest is wet. The temperature of the modules of the dry section is almost isothermal with difference between first module surface temperature and last dry module temperature is less than 1°C. The wet section temperature difference between first and last wet modules is less than 1.6°C. The developing turbulent flow correlation of average Nusselt in terms of Reynolds and Greatz number over each section was used to estimate the internal convection coefficient [20]. This approach has been used by Pierres *et al.* [21].

The internal heat convective transfer coefficient for the wet part of the cooling channel can be obtained by the following equation:

$$h_{i-wet} = h_{i-dry} \times C_{d-w} \quad (10)$$

where h_{i_dry} is the internal heat convective transfer coefficient for the dry part and C_{d-w} is given by

$$C_{d-w} = \frac{dh}{dT} \times \frac{1}{cp_m} \quad (11)$$

Hence, dh/dT is the change in the enthalpy with respect to the change in temperature and it is obtained by the following correlation based on the cold surface temperature (T_c) [5]:

$$\frac{dh}{dT} = 3.5625 \times 10^{-7} \times T_c^4 + 3.646 \times 10^{-5} \times T_c^3 + 0.0006939 \times T_c^2 + 0.5472 \times T_c + 1.667 \quad (12)$$

Finally, the specific heat of moist air is determined by the following equation:

$$Cp_m = Cp + w \times Cp_w \quad (13)$$

The amount of water condensate obtained during a period of time t is given by

$$m_{cond} = \dot{m} \times (w_{a-in} - w_{a-out}) \times t \quad (14)$$

where w is air humidity ratio in kg (water)/kg (air), Cp_w is the water vapor specific heat capacity in $J\,kg^{-1}\,K^{-1}$.

Int. J. Energy Res. 2012; **36**:963–974 © 2011 John Wiley & Sons, Ltd.
DOI: 10.1002/er

The channel flow model will be integrated with the solar still humidification model developed by Alsaidi *et al*. [22]. The solar distiller air flow and brakish water basin are modeled as lumped quasi-static systems. The distiller model predicts well the exit air temperature and humidity from the distiller. It assumes a well-insulated solar distiller with a lumped glass temperature. In addition to that, the solar distiller model assumes that air is a low-capacity fluid and neglects the spatial and transient variation in the temperature of air. The model is based on a set of energy balances developed for the distiller glass, the air flow, the water in the basin and the water vapor flow. The experimentally validated solar still model of Alsaidi *et al*. [22] predicts the humidified air exit temperature and humidity for an open cycle. In our study, the air input to the solar distiller model is not the ambient air, but is a mixture of fresh air from outside and return air from the distiller. This will increase the water content of the air leaving distiller to the TEC channels.

4. NUMERICAL SOLUTION

The set of energy balance equations of the three system units of TEC modules, cooling channel and solar distiller described in the previous section will be solved numerically to predict the exit air conditions from the cooling channel. Input parameters to the distiller unit are time-dependent ambient air temperature and humidity and intensity of solar radiation. Given ambient and solar conditions and mixing ratio of re-circulated air flow to ambient flow, the solar distiller model predicts the temperature and the water content of the air exiting the solar distiller and entering the TEC channel.

Every TEC module is characterized by restrictions on its operational parameters, which dictate the accurate selection of the optimal cooling module for the cooling application. Given the characteristic TEC values as provided by manufacturer on I_{max}, U_{max}, Q_{max} and ΔT_{max} at the hot side temperature (T_h), we obtain other design parameters. These include the number of thermocouples (Nb) in the thermoelectric cooling module, the GF of the thermoelectric element (Gf), the width, length and thickness of the TEC module, and its overall thermal resistance. The overall thermal resistance is measured experimentally and a statistical correlation for this resistance is developed for use in our model in terms of the two main governing parameters: the input electric current and the ambient environment temperature. In determining the thermoelectric modules' parameters, each TEC module is treated as a lumped system, and its parameters are coupled with the next one, through the channel airflow where the air exiting after one module is considered as inlet air input to the next channel section containing the following module. Therefore, the thermal and electrical parameters will not be the same for all the thermoelectric modules in the cooling channel because each one is working under specifically different conditions.

Based on the mathematical formulation presented above, we have for each module 10 equations in 10 unknowns which are T_c, T_h, Q_c, Q_h, P, U, h_{a_out}, α, k and R_e. The Gauss–Seidal iterative method will be used to solve for the 10 unknowns. Given the mass flow rate of the air entering the thermoelectric cooling channel and the TEC module input electric current, we assume a cold side temperature T_c. Using Equation (9), the temperature and the enthalpy of the air exiting the thermoelectric cooling module T_{a-out} and h_{a_out} are obtained. The cooling capacity can then be found from Equation (7). By equating Equations (2) and (8) of the heat dissipated on the hot side, and substituting α, k and R_e with their correlations given in Equations (5a) and (5b), we can then calculate the value of the average module temperature T_m. As a result, the hot side temperature T_h and the new updated values for the thermoelectric cooling module characteristics α, k and R_e can be obtained in terms of the new calculated module average temperature. We can re-calculate the total amount of heat dissipated at the hot side Q_h by Equation (8). The final step in the iterative method is calculating a new updated value for the thermoelectric module cold side temperature T_c from Equation (1) and check for convergence. Convergence is attained when difference in temperature is less than 0.00001°C after which we calculate the electric power consumption and the COP of the module. The procedure is repeated on the following modules until exit air conditions from the channel are obtained. Finally, from the properties of the humid air entering the cooling channel and that leaving the channel, we can evaluate the total amount of condensate produced. A flow chart showing the iterative method is presented in Figure 2.

The model of the solar distiller predicts the exit air temperature and humidity from the distiller for varying inlet conditions. The presented numerical model predicts the hourly temperature and the humidity of the air leaving the cooling channel, the variation of the air temperature through the channel, the thermoelectric modules hot and cold side temperatures and their corresponding heating and cooling capacities as well as the electric power consumption and the amount of collected water condensate.

5. EXPERIMENTAL METHODOLOGY

This section presents the experimental setup used for validating the developed thermoelectric cooling simulation model predictions as well as for testing the performance of the cooling system and condensed

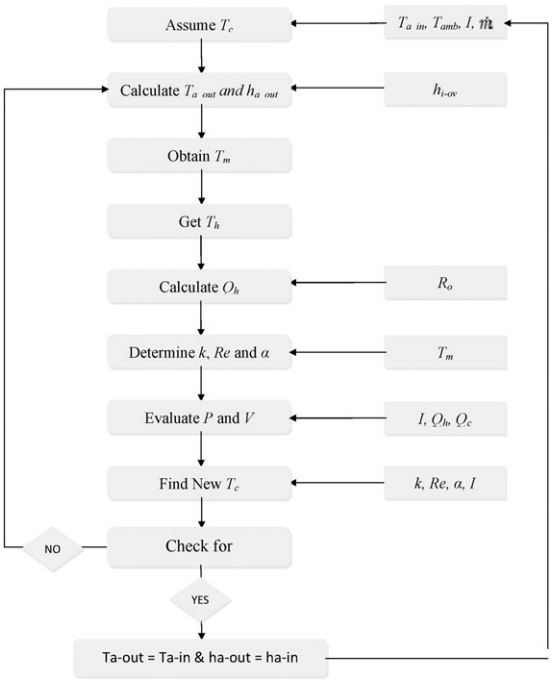

Figure 2. Iterative method flow chart.

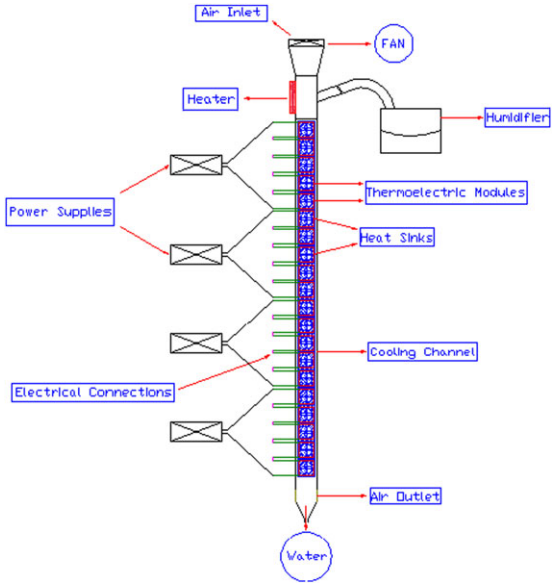

Figure 3. Experimental system unit.

Table I. TEC1-12714 performance specifications.

TEC performance parameters' specifications		
T_h (hot side temperature in °C)	27	50
ΔT_{max} (temperature difference in °C)	68	76
U_{max} (voltage in Volts)	14.8	16.6
I_{max} (electric current in Amperes)	14	14
Qc_{max} (cooling capacity in Watts)	135	148
AC resistance (Ω)	0.95	1.06

water output under different operational and ambient conditions.

Figure 3 shows a schematic of the TEC channel prototype in addition to a humid air source, a heater, electric power supplies, 12 W AC supply fan rated at a maximum flow rate of 54 cfm, and a water collection graded-beaker. The cooling channel is 120 cm long with a 7 cm × 5 cm cross-sectional area. Twenty TEC1-12714 thermoelectric cooling modules of 5 cm × 5 cm area are mounted on one side along the length of the channel at 1 cm gap between the modules. The three other sides were insulated with fiberglass sheet. The characteristics of the TEC modules are given in Table I. The system is placed in a climatic chamber with advanced temperature and relative humidity level control system. The humid air source replaces the solar still in providing supply air at high humidity content to the thermoelectrically cooled channel, and the electric heater is used to control the channel inlet air temperature. In addition, the electric power supply (DC voltage source) replaces the PV system and provides the electricity needed to power the TEC modules to pump the needed cooling capacity. The variation of the air mass flow rate to the channel is regulated using a damper. This climatic air is mixed with the water vapor sprayed by the humidifier and heated using the electric heater to reach the desirable input air conditions to the cooling channel. The heat emitted at the hot side of the modules is removed using aluminum heat sinks with integrated DC cooling fans. Four electric power supplies are used to feed the thermoelectric modules such that each power supply feeds five modules connected in series with a constant DC voltage.

The temperatures of the air and the cold and hot side temperatures of the TEC modules were measured using K-type thermocouples of accuracy ±3°C at six positions in the channel including inlet and exit temperatures. A humidity sensor was used to record the humidity of the air entering the cooling channel with an accuracy of ±1%, and a flow meter was used to measure the air flow rate in the channel by recording the velocity of the air with an accuracy of $\pm 0.01\ m\ s^{-1}$. Moreover, a heat flux meter of 0.6-s response was equipped to measure the heat flux emitted at the hot side of the thermoelectric cooling modules. The water condensate was collected in a beaker placed on an accurate digital scale to monitor the weight of collected water. The digital precision balance is a maximum scale reading of 3500 g and an accuracy of 0.01 g. Preliminary experiments were carried out to determine the overall thermal resistance at the hot side of the thermoelectric modules by recording the heat flux released at the hot side of the modules as well as the

Int. J. Energy Res. 2012; **36**:963–974 © 2011 John Wiley & Sons, Ltd.
DOI: 10.1002/er

temperature. The heat flux is recorded in Volts where each 1.77 μV is equivalent to 1.0 W m^{-2} heat flux.

Several experiments were performed for different mass flow rates of inlet air, electric current input to the TEC modules, and different channel inlet air temperature and humidity. The electric current varied between 1 and 3.5 A, channel air mass flow rate was varied between 0.005 and 0.012 kg s^{-1}, inlet air temperature to the cooling channel varied between 25 and 34°C, inlet air relative humidity varied between 70 and 90%, and ambient air varied between 25 and 34°C. The variation in the air temperature along the thermoelectric cooling channel was recorded, and the amount of water condensate generated was collected and measured at intervals of 1 h during the experimentation sessions.

6. MODEL VALIDATION WITH EXPERIMENTAL RESULTS

Figure 4 shows the amount of water condensate collected per hour as a function of (a) electric current, (b) air mass flow rate and (c) inlet air temperature for experimentally measured and numerically predicted values. The simulation model predicts well the amount of water condensate produced by the new integrated system over hourly intervals with a maximum relative error less than 8.3%. The water condensate increases with channel air mass flow rate in the range of experiments from 0.005 to 0.01 kg s^{-1}. Figure 5 presents the variation in the air temperature through the thermoelectric cooling channel recorded at six different heights: at the channel inlet (T_1), between the fourth and the fifth thermoelectric cooling modules (T_2), between the eighth and the ninth modules (T_3), between the 12th and the 13th modules (T_4), between the 16th and the 17th modules (T_5) and at the channel outlet (T_6), at different electric current input to the thermoelectric modules for the case of 28°C ambient temperature, 0.01 kg s^{-1} air mass flow rate at 30°C inlet air temperature. Our thermoelectric cooling channel simulation model predicted well the variation in the air temperature through the thermoelectric cooling module with a maximum relative error less than 2.4% (±0.55°C).

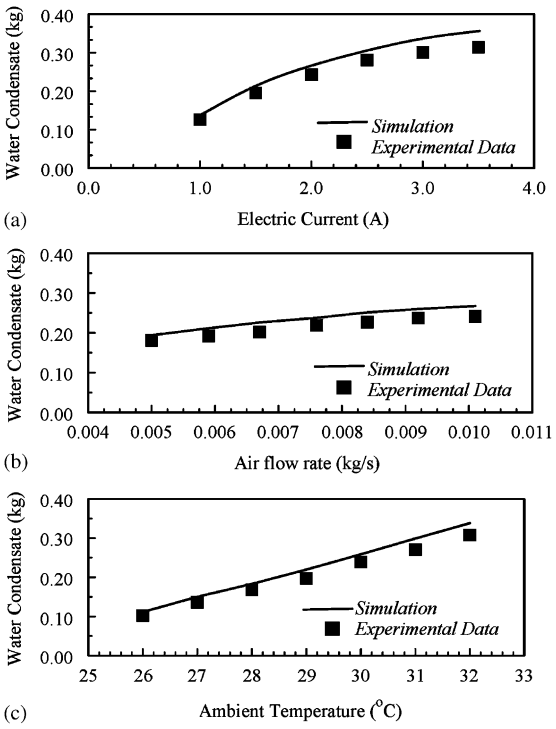

Figure 4. Plots of (a) water condensate versus electric current as predicted by the model and recorded experimentally, (b) water condensate versus mass flow rate as predicted by the model and recorded experimentally and (c) water condensate versus inlet air temperature as predicted by the model and recorded experimentally.

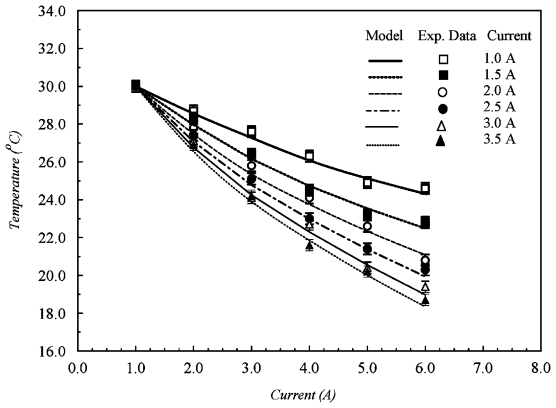

Figure 5. Air temperature variation as measured experimentally and predicted by modeling for different electric current inputs at 0.01 kg s^{-1} air mass flow rate, 28°C ambient temperature and 30°C inlet air temperature. The symbols T1 to T6 refer to position of TEC modules along the channel height.

7. CASE STUDY

To assess the viability of sizing and using the proposed integrated thermoelectric–PV system in meeting the fresh water needs in the Lebanese humid climate, a case study of a typical residential space of 80 m^2 is considered. The system will be sized to provide at least 10 L of fresh water over a period of operation from 10:00 am to 7:00 pm during the summer months from June till October. An optimization problem is formulated such that the energy consumption of the unit is dictated by fresh water demand and the availability of electrical energy supplied by the PV system [23].

The integrated system design, operation and optimization are performed for the Beirut local humid weather conditions. The system is sized such that multiple TEC channels are utilized, each with a length of 120 cm and a cross-sectional area of 7 cm × 5 cm. Twenty thermoelectric cooling modules are mounted per each cooling channel as per the channel description in the previous section. Moreover, the thermoelectric cooling modules use solar PV modules for their electrical input. The number of channels needed and their associated number of thermoelectric cooling modules are dictated by two main constraints as follows:

- The availability of 1 kW of solar PV modules capacity.
- The amount of fresh water produced over the 10 h of daily operation.

A solar distiller of 1.2 m^2 area with a constant air mass flow rate of 0.15 $kg\,s^{-1}$ is integrated with the TEC-PV system to provide desired humid air flow to the cooling channels and enhance fresh water production. The solar distiller air flow is partially recirculated while only a fraction of this flow is drawn from ambient air equal to the dehumidified air stream supplied to the TEC channels (see Figure 1). This modification helps in increasing the system fresh water output by increasing further the water content in the supply air to the dehumidifying TEC channel.

The optimization problem is controlled by the air mass flow rate of the TEC channels and the electric current input to the TEC modules. A minimum of five TEC channels is needed to produce the 10 L of water over 10 h of operation. Many simulations were performed at different air mass flow rates from 0.005 to 0.02 $kg\,s^{-1}$ to find the optimal mass flow rate to be introduced to the TEC channels from the solar distiller with respect to the electrical energy consumption of the system. Figure 6 shows the variation of water condensate produced with the variation in the air mass flow rate in the TEC channels for different electric current input in the month of August. The amount of water produced increases with the increase in the air mass flow rate until the air mass flow rate reaches 0.0155 $kg\,s^{-1}$ per channel. For air mass flow rates higher than 0.0155 $kg\,s^{-1}$, a decrease is exhibited in the amount of fresh water produced by the system. Based on these results, an air mass flow rate of 0.0155 $kg\,s^{-1}$ will be adopted per cooling channel.

The optimal electric current input to the thermoelectric cooling modules is selected such that a minimum of 10 L of fresh water is obtained at the maximum electrical energy available from the PV system. The first step in solving for the optimal settings is to calculate the maximal electrical energy generated by the 1-kW PV system in the Lebanese summer humid climate. This is governed by the solar irradiation intensity and the ambient air properties that vary significantly from one month to another. As a result, this maximal energy is calculated for each of the five summer months from June till October. Simulations were performed while varying the electrical current input to the TEC modules with a step of 0.1 A in the range of 1.0–3.0 A. Based on the electrical energy consumption results and the amount of fresh water collected, we can determine the optimal electrical current input to the system for each month. Figure 7(a, b) shows the amount of fresh water produced and the PV

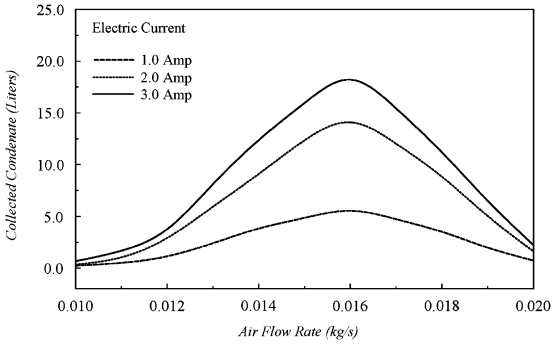

Figure 6. Variation in water condensate with the variation in air mass flow rate under different electric current supply to the system in August.

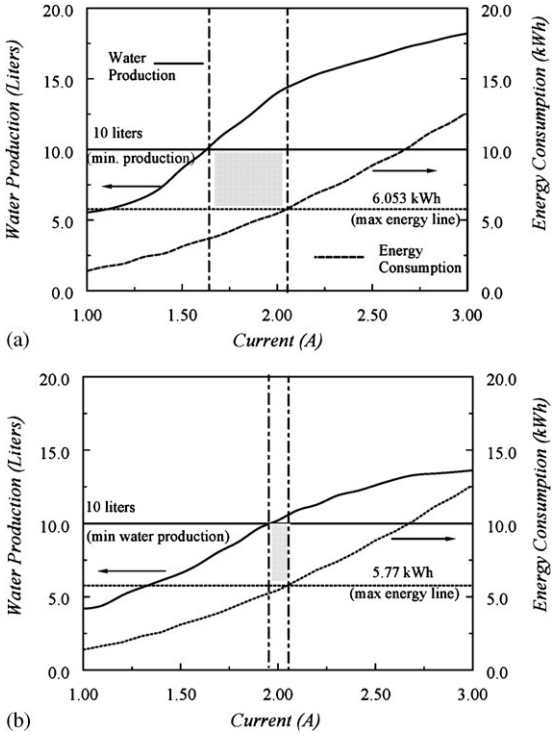

Figure 7. (a, b) The amount of fresh water produced and the PV power consumption as a function of electric current input to the TEC modules for (a) August and (b) September.

Int. J. Energy Res. 2012; **36**:963–974 © 2011 John Wiley & Sons, Ltd.
DOI: 10.1002/er

power consumption as a function of electric current input to the TEC modules for (a) August and (b) September. On the same plots, the constraint values for minimum water production and maximum power consumption are indicated. It is clear that the month of August provides wider operating range (shown by the shade rectangle borders in the figures) for the system to produce more than 10 L per day, while in September, the operating margin for current input is small (1.95 to 2.05 A). Owing to the constraint by design of a maximum of 1 kW available PV power, the optimal current value is not necessarily at the maximum COP of the module since it has to meet the 10-L water production constraint.

Performing the simulations over all the summer months leads to optimal electric current input values of 2.2 A module^{-1} for the month of June, 2.1 A module^{-1} in July, and 2.0 A module^{-1} for August, September and October. The selected current input values provide the needed cooling capacity, produce the desired fresh water, and meet the constraints at acceptable thermoelectric cooling system COP over the 10 h of system operation per day.

8. RESULTS AND DISCUSSION

The hourly and overall performance of the proposed PV-powered TEC channel integrated with solar distiller to produce at least 10 L of fresh water per day are presented in this section.

Table II presents the hourly amount of fresh water produced during the summer months showing how the system met its goal of producing at least 10 L of fresh water during the 10 h of operation per day. The maximum amount of fresh water produced is attained between 3:00 and 6:00 pm for 5 months and the amount of fresh water produced ranged from about 14.09 L day^{-1} in August to about 10.06 L day^{-1} in October. This is mainly due to the humid ambient air conditions and the higher solar radiation intensity, which vary significantly from one month to another. Figure 8 compares the total amount of fresh water collected for the PV-powered TEC system operation with and without integration with the solar distiller. The requirement for producing 10 L of water cannot be met for all the months without the humidification process through the solar distiller. The solar distiller enhances the water condensate yield by increasing the water content of the air introduced to the TEC channels. The amount of water condensate produced due to the integration of the solar distiller in the process has increased from 4.72 to 14.09 L in August and from 2.31 to 10.06 L in October.

Figure 9 shows (a) the cooling capacity pumped by the thermoelectric cooling modules per day and (b) the

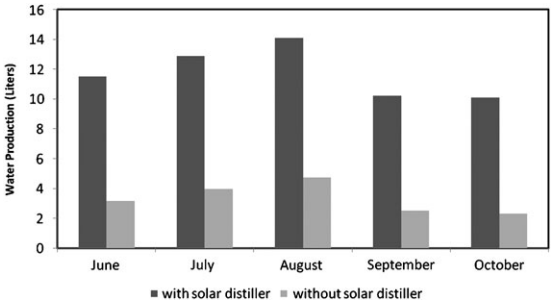

Figure 8. Total fresh water production over 10 h of the PV-powered TEC system with and without the solar distiller.

Table II. Hourly and total amount of condensed water over 5 months.

	Month				
	June	July	August	September	October
Electric current input (A)	2.2	2.1	2	2	2
Hour	Fresh water production (mL)				
10:00 am	714.2	659.8	844.2	547.2	516.3
11:00 am	914.9	796.5	951.0	581.7	727.3
12:00 pm	1028.9	1016.6	1042.1	781.1	923.3
1:00 pm	1172.9	1136.4	1303.8	958.2	1034.3
2:00 pm	1285.3	1328.6	1404.8	1025.2	1215.7
3:00 pm	1296.4	1496.5	1528.1	1292.8	1310.5
4:00 pm	1379.9	1654.4	1546.4	1345.2	1342.2
5:00 pm	1352.0	1647.9	1937.4	1308.2	1168.6
6:00 pm	1272.1	1617.5	1861.2	1255.8	1025.3
7:00 pm	1077.2	1536.7	1672.6	1113.2	803.4
Total (mL)	11 494.1	12 891.3	14 091.6	10 208.8	10 067.4

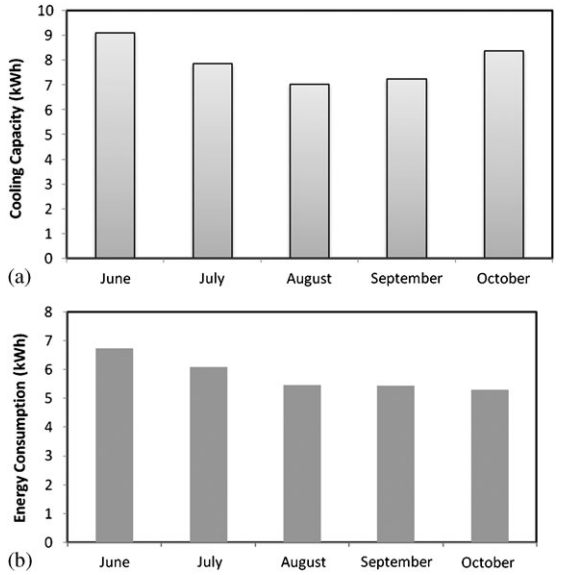

Figure 9. (a, b) Plots of (a) the cooling capacity pumped by the thermoelectric cooling modules per day and (b) the associated system energy consumption from the PV in kWh day^{-1} over the summer months.

associated system energy consumption from the PV in kWh day^{-1} over the summer months. The cooling capacity reaches its maximum in June with about 9.07 kWh day^{-1} while decreases to about 7.02 kWh in August. The energy consumption varies from a minimum of 5.32 kWh day^{-1} (October) to a maximum value of 6.73 kWh day^{-1} (June). A maximum system COP is attained in October at a COP of 1.52. Thus, although the amount of fresh water produced in October is the lowest among all the five months studied, it exhibits the highest COP with minimum electrical input. This is due to the relatively lower ambient temperature values (sink temperature) in October compared with the other months. This is consistent with the TEC modules performance characteristics where the cooling capacity pumped is inversely proportional to the temperature gradient between the two thermoelectric sides. The energy intensity of our proposed integrated solar distiller with PV-powered TEC channel system is found minimum at 0.387 kWh L^{-1} in August and maximum in June at 0.586 kWh L^{-1}. These values are better than the vapor-compression atmospheric water extraction systems that consume about 0.7 kWh L^{-1} of fresh water [22,24].

9. CONCLUSIONS

A new integrated solar-driven thermoelectric cooling system for air dehumidification and fresh water production was presented and experimentally validated in this study. The system is totally powered by renewable energy sources. A model of the integrated system is developed and is validated experimentally. The air flow rate, air inlet conditions and electric current input to the TEC modules are the controlling parameters for optimal system operation to meet desired need of water condensate at lowest power input from the PV system.

A case study is presented demonstrating the feasibility of implementing the integrated solar distiller PV powered TEC channel system in Beirut climate for producing at least 10 L of water per day over the summer months. The system is considered practical for stand-alone remote areas applications in the humid climates and in the areas where the electrical supply is intermittent.

NOMENCLATURE

A	= area (m^2)
CCD	= charge coupled device
COP	= coefficient of performance
C_p	= specific heat coefficient at constant pressure (J kg^{-1} K^{-1})
C_{p_w}	= water vapor specific heat capacity (J kg^{-1} K^{-1})
DC	= direct current
DNA	= deoxyribonucleic acid
Gf	= geometry factor (cm)
h	= enthalpy (J kg)
h_i	= internal heat convective transfer coefficient (W m^{-2} K^{-1})
I	= electric current (A)
k	= thermal conductance of the module (W K^{-1})
LED	= light emitting diode
m	= mass (kg)
$\dot{m}$	= mass flow rate (kg s^{-1})
Nb	= number of thermocouples
P	= electric power (W)
PV	= photovoltaic
Q	= thermoelectric net heat (W)
R	= thermal resistance (K W^{-1})
R_e	= electrical resistivity (Ω)
RH	= relative humidity, (%)
T	= temperature (°C)
U	= voltage difference (V)
w	= humidity ratio (kg H_2O kg^{-1} of air)
ΔT	= temperature difference (°C)

Greek

α	= Seebeck coefficient (V K^{-1})

Subscripts

a	= air
amb	= ambient

Int. J. Energy Res. 2012; **36**:963–974 © 2011 John Wiley & Sons, Ltd.
DOI: 10.1002/er

c	= cold
cond	= condensate
dist	= distiller
dry	= dry conditions
e	= thermoelectric element
h	= hot
i	= internal
in	= input
m	= module
n	= n-type semiconductor
out	= output
p	= p-type semiconductor
wet	= wet conditions

ACKNOWLEDGEMENTS

The financial support of the Munib Masri Institute for Energy and Natural Resources, the ASHRAE Senior Project Award 2010-11, District Cooling PRO Engineering of UAE, and the Qatar Chair in Energy Studies Endowment Fund are all highly acknowledged.

REFERENCES

1. /SANDIA 2003/ Miller JE, Review of Water Resources and Desalination Technologies, Sandia National Laboratories, Albuquerque *Sand 2003-0800*, 2003.
2. Mezher T, Fath H, Abbas Z, Khaled A. Techno-economic assessment and environmental impacts of desalination technologies. *Desalination* 2011; **266**(1–3):263–273.
3. Huang BJ, Chin CJ, Duang CL. A design method for thermoelectric cooler. *International Journal of Refrigeration* 2000; **23**:208–218.
4. Khattab NM, El Shenawy ET. Optimal operation of thermoelectric cooler driven by solar thermoelectric generator. *Energy Conversion and Management* 2006; **47**:407–426.
5. Kuehn HT, Ramsey JW, Threlkeld JL. *Thermal Environmental Engineering*, Chapter 7 (3rd edn). Prentice-Hall Inc: New York, 1998.
6. Nolwenn LP, Matthieu C, Luo L, Fraisse G. Coupling of thermoelectric modules with a photovoltaic panel for air pre-heating and pre-cooling application; an annual simulation. *International Journal of Energy Research* 2008; **32**:1316–1328.
7. Charoenporn L, Wiset L, Atthajariyakul S. Evaluation of the thermal comfort of a thermoelectric ceiling cooling panel (TE-CCP) System. *Journal of Electronic Materials* 2009; **38**(7):1472–1477.
8. Bansal PK, Martin A. Comparative study of vapour compression, thermoelectric and absorption refrigerators. *International Journal of Energy Research* 2000; **24**(2):93–107.
9. Riffat SB, Xiaoli MA. Improving the coefficient of performance of thermoelectric cooling system. *International Journal of Energy Research* 2004; **28**(12):753–768.
10. Riffat SB, Xiaoli MA. Optimum selection (design) of thermoelectric modules for large capacity heat pump applications. *International Journal of Energy Research* 2004; **28**(14):1231–1242.
11. Chen K, Gwilliam SB. An analysis of the heat transfer rate and efficiency of TE (thermoelectric) cooling systems. *International Journal of Energy Research* 1996; **20**(5):399–417.
12. Yu-Wei C, Cheng CH, Wu WF, Chen SL. An experimental investigation of thermoelectric air-cooling module. *World Academy of Science, Engineering and Technology* 2007; **33**:128–133.
13. Cosnier M, Fraisse G, Luo L. An experimental and numerical study of a thermoelectric air-cooling and air-heating system. *International Journal of Refrigeration* 2008; **31**:1051–1062.
14. Gillot M, Jiang L, Riffat S. An investigation of thermoelectric cooling devices for small-scale space conditioning applications in building. *International Journal of Energy Research* 2010; **34**(9): 776–786.
15. Dai YJ, Wang RZ, Ni L. Experimental investigation and analysis on a thermoelectric refrigerator driven by solar cells. *Solar Energy Materials and Solar Cells* 2003; **77**(4):377–391.
16. Vian JG, Astrain D, Dominguez M. Numerical modeling and a design of a thermoelectric dehumidifier. *Applied Thermal Engineering* 2002; **22**(4): 407–422.
17. Tsai HL, Lin JM. Model building and simulation of thermoelectric module using matlab/simulink. *Journal of Electronic Materials* 2010; **39**(9):2105–2111.
18. Yang B, Ahuga H, Tran N. Thermoelectric technology assessment application to air conditioing and refrigeration. *HVAC&R Research* 2007; **14**(5): 635–653.
19. Rowe DM. Modeling of thermoelectric cooling systems. *CRC Handbook of Thermoelectrics*, Chapter 55. CRC Press Inc: Boca Raton, U.S.A., 1995; 677–683.
20. Lienhard V, John H. *A Heat Transfer Textbook* (3rd edn). Phlogiston Press: New York, 2003.
21. Nolwenn LP, Cosnier M, Luo L, Fraisse G. Coupling of thermoelectric modules with a photovoltaic panel for air pre-heating and pre-cooling

application; an annual simulation. *International Journal of Energy Research* 2008; **32**:1316–1328.
22. Alsaidi A, Ghaddar N, Ghali K. Experimental and theoretical study of an optimized integrated solar desalination and air-conditioning unit. *International Journal of Green Energy* 2011; **8**(1):81–99.
23. Astrain D, Vian JG, Dominguez M. Increase of COP in the thermoelectric refrigeration by optimization of heat dissipation. *Applied Thermal Engineering* 2003; **23**:2183–2200.
24. Skywater®, 2009. Available from: http://islandsky.com/products/home-and-office-water-making-machine.

Int. J. Energy Res. 2012; **36**:963–974 © 2011 John Wiley & Sons, Ltd.
DOI: 10.1002/er